

High-frequency magnetic properties of dysprosium orthoferrite

A. M. Balbashov, A. A. Volkov, S. P. Lebedev, A. A. Mukhin, and A. S. Prokhorov

Institute of General Physics, USSR Academy of Sciences

(Submitted 29 July 1984)

Zh. Eksp. Teor. Fiz. **88**, 974–987 (March 1985)

The high-frequency magnetic properties [$\mu'(\nu)$, $\mu''(\nu)$] of DyFeO_3 were investigated in the frequency band $\nu = 5\text{--}33\text{ cm}^{-1}$ and at temperatures 4.2–600 K. Temperature dependences were obtained for two antiferromagnetic-resonance modes, viz., the resonance frequencies $\nu_0^{(1,2)}$ ($\nu_0^{(1)} = 12.67\text{ cm}^{-1}$ and $\nu_0^{(2)} = 17.0\text{ cm}^{-1}$ at $T = 300\text{ K}$), the linewidths $\Gamma^{(1,2)}$, and the contributions $\Delta\mu_0^{(1,2)}$ made to the static magnetic permeability. Anomalies of the indicated quantities were observed at a Morin-type phase-transition point (a minimum on the temperature dependence of the frequency $\nu_0^{(2)}(T)$ of the quasiantiferromagnetic mode, and discontinuities in $\Gamma^{(1,2)}$ and $\Delta\mu_0^{(1,2)}$). A theoretical analysis within the framework of a simple model that uses the Landau-Lifshitz equations and a system thermodynamic potential renormalized by the Dy-Fe interaction has shown that the observed $\nu_0^{(1,2)}(T)$ and $\Delta\mu_0^{(1,2)}(T)$ dependences are well described by this model and agree with the static magnetic properties of DyFeO_3 . They can be used to obtain additional information on the magnetic characteristics of the system, such as the anisotropy constants, the Fe-subsystem transverse susceptibility, and others.

1. INTRODUCTION

Rare-earth orthoferrites (RFeO_3) are weak ferromagnets with rhombic symmetry, in which the exchange interaction between the rare-earth ions and the iron ions governs the great diversity of their magnetic properties. The interest in orthoferrites is due for the most part to the various orientational phase transitions (PT) to which they are subject and near which strongly pronounced singularities are observed in both the static¹ and dynamic²⁻⁴ properties of these crystals.

Active research into the high-frequency magnetic properties of rare-earth orthoferrites, particularly antiferromagnetic resonance (AFMR), are being undertaken of late.²⁻⁹ The orthoferrite unit cell contains four RFeO_3 molecules. The Fe subsystem has accordingly four modes of homogeneous magnetic oscillations, of which two (high-frequency or exchange modes) have frequencies $\nu \sim 10^3\text{ cm}^{-1}$, and the others are respectively the quasiferromagnetic (1) (σ mode) and the quasiantiferromagnetic (2) (γ mode) of the AFMR.¹⁰⁻¹² The frequencies of the last two lie in the submillimeter band. Their characteristic features are that in the quasiferromagnetic mode the ac components of the resultant magnetic moment are orthogonal to its dc component (just as in a ferromagnet), whereas in the quasiantiferromagnetic mode they are aligned with the dc component.¹¹

There are also rare-earth modes whose frequencies ($\nu \sim 0.1\text{--}10^2\text{ cm}^{-1}$) are determined by the splitting of the principal multiplet of the rare-earth ion in the crystal field, in the external magnetic field, and in the effective field produced by the Fe subsystem. We note that by virtue of the exchange and dipole R-Fe interactions the oscillations of the Fe and R subsystems are coupled.

When the temperature is lowered, the R-Fe interaction gives rise to a strong temperature dependence of the thermodynamic-potential parameters (of the effective anisotropy constants etc.), causing peculiar temperature dependences of

the AFMR frequencies. This is particularly pronounced in orientational PT, when softening of the corresponding mode takes place at the transition points. This softening of the quasiferromagnetic mode, determined by the anisotropy energy in the ac plane, was observed in TmFeO_3 (Ref. 3) and ErFeO_3 (Refs. 3 and 4) following spontaneous reorientation, via two second-order phase transitions, of the weakly ferromagnetic moment from the c axis to the a axis. This spin reorientation is most prevalent in orthoferrites.¹

Another type of orientational PT is realized in dysprosium orthoferrite (DyFeO_3), which is the only unsubstituted orthoferrite in which, when the temperature is lowered, an orientational phase transition takes place at $T_M = 40\text{--}50\text{ K}$ from the weakly ferromagnetic phase $\Gamma_4(G_x F_z)$ into the antiferromagnetic phase $\Gamma_1(G_y)$ (Morin-type orientational PT).^{1,13,14} In the course of this transition the antiferromagnetism vector \mathbf{G} of the Fe^{3+} ions is reoriented in the ab plane of the crystal from the a to the b axis. In DyFeO_3 , unlike the previously investigated orthoferrites (TmFeO_3 , ErFeO_3 and others), the PT should be accompanied by a softening of the frequency of the quasiantiferromagnetic mode determined by the anisotropy energy in the ab plane. At room temperature, the quasiantiferromagnetic-mode frequency $\nu_0^{(2)}$ lies higher than the frequency $\nu_0^{(1)}$ of the quasiferromagnetic mode,⁴ so that the frequencies of these modes can cross with decreasing temperature. We note also that since the spin reorientation in DyFeO_3 proceeds via first-order PT,¹⁴ this should manifest itself in the behavior of its high-frequency characteristics at the Morin point.

The purpose of the present paper is the following:

a) Investigate the transmission spectra of DyFeO_3 single crystals in the frequency range $\nu = 5\text{--}33\text{ cm}^{-1}$ at temperatures from 4.2 to 600 K and determine the temperature dependences of the AFMR frequencies, of the line widths, and of the contributions of the corresponding modes to the static magnetic permeability.

b) Study the anomalies of the high-frequency magnetic

characteristics of DyFeO₃ at a Morin-type PT point and compare them with the static magnetic properties of the system; ascertain the role of the Dy³⁺ ion subsystem in the AFMR region.

2. EXPERIMENT

We investigated DyFe₃ single crystals grown by non-crucible zone melting and radiation heating.¹⁵ The samples were cut from the ingot and finished by optical methods to form plane-parallel *a*-cut plates ~1 cm square in cross section and 0.5 to 1.5 mm thick.

A submillimeter "Epsilon" BWO spectrometer²⁾ (Ref. 16), with a frequency range 5 to 33 cm⁻¹ at zero external magnetic field, was used to measure the transmission spectra of the DyFeO₃ plates at two polarization orientations of the rf magnetic field, **h**||*c* and **h**||*b*. We used a standard measurement procedure which we employed many times in the past¹⁷ to study the properties of nonmagnetic dielectrics at submillimeter wavelengths. In this procedure a simple optical system is used to transmit directly through the plane-parallel plate a beam of monochromatic linearly polarized radiation whose frequency is automatically varied during the measurements. The sample transmission spectrum *T*(ν) is calculated as the ratio of the receiver signal with and without the sample in the measurement channel. The measurements are carried out in free space. The crystallographic axes of the samples are oriented relative to the polarization of the working radiation by birefringence. The sample is rotated between perpendicularly oriented polarizers around the axis normal to its surface, until a minimum receiver signal is obtained. One of the principal axes of the dielectric indicatrix is then directed along the polarization of the radiation.

The main quantities characterizing our DyFeO₃ experiments were: signal/noise ratio ~10⁵, frequency resolution ~0.001 cm⁻¹, radiation polarization ~99.99%, time to record a *T*(ν) spectrum consisting of 100 points ~10 s, error in sample-axes setting not worse than 1°, range of sample tem-

peratures from 4.2 to 600 K, and temperature-stabilization error in the range from 0.1 to 1 K, depending on the absolute value of the temperature.

Figure 1 shows two fragments of *T*(ν) dependences measured at room temperature. A common feature of such spectra in the entire frequency range from 5 to 33 cm⁻¹ is the presence of periodic oscillations that result from interference of the waves within the plane-parallel plates and demonstrate thereby the very high transparency of DyFeO₃ to submillimeter radiation. Besides the oscillations due to interference, the *T*(ν) spectra show two pronounced features—narrow resonance absorption lines at 12.6 cm⁻¹ (at **h**⊥*c*) and 17.0 cm⁻¹ (at **h**||*c*). The depths of the resonance minima are found to be very sensitive to the excitation conditions, and it can be seen from Fig. 1 that only one of the lines is observed when **h** is oriented exactly along the *c* axis, and only the other at **h**⊥*c*. These conditions for the excitation of the observed modes coincide with the conditions for the excitation of the quasiferromagnetic (**h**⊥*c*) and quasiantiferromagnetic modes (**h**||*c*) of the AFMR in the orthoferrite in the $\Gamma_4(G_x F_2)$ phase, thus pointing to their magnetic origin. Further evidence is the increase of the frequency of the lines observed by us in the dc magnetic field **H**||*c*.

To determine the parameters of the observed AFMR modes, we reduced the *T*(ν) spectra by least squares, using a simple damped harmonic oscillator as the model for the magnetic permeability $\mu(\nu) = \mu'(\nu) - i\mu''(\nu)$, which we specified in the form

$$\mu(\nu) = 1 + \Delta\mu_0 \nu_0^2 / (\nu_0^2 - \nu^2 + i\Gamma\nu), \quad (1)$$

where ν is the radiation frequency, ν_0 is the resonant frequency, Γ is the line width, and $\Delta\mu_0$ is the contribution of the mode to the static magnetic permeability. The *T*(ν) dependence was assumed specified by the familiar optical expression for the coefficient of transmission of a plane wave through a layer of thickness *d*₁ and having besides μ also a dielectric constant $\epsilon(\nu) = \epsilon'(\nu) - i\epsilon''(\nu)$ (Ref. 18):

$$T(\nu) = E \left[\frac{(1-R)^2 + 4R \sin^2 \psi}{(1-ER)^2 + 4RE \sin^2(\psi + 2\pi n d\nu/c)} \right], \quad (2)$$

$$E = \exp(-4\pi k d\nu/c), \quad R = \frac{(a-1)^2 + b^2}{(a+1)^2 + b^2},$$

$$\psi = \arctg \left[\frac{2b}{(a^2 + b^2 - 1)} \right], \quad n - ik = (\epsilon\mu)^{1/2}, \quad a + ib = (\mu/\epsilon)^{1/2},$$

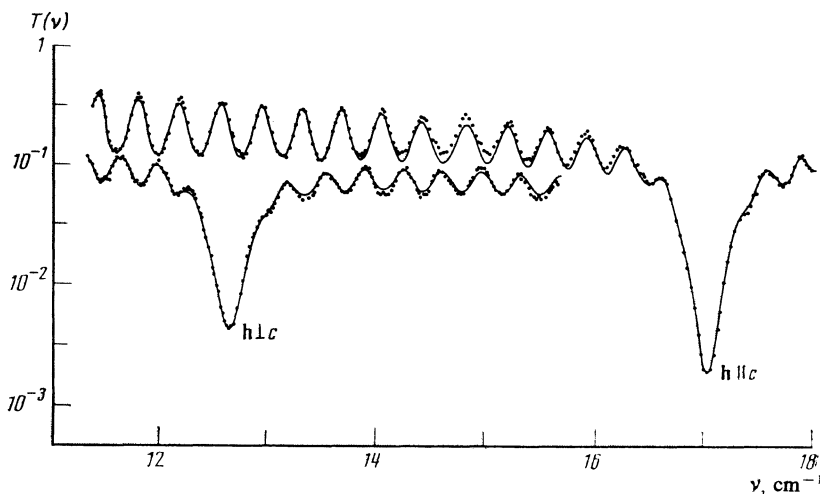


FIG. 1. Transmission spectra of DyFeO₃ at room temperature at two polarizations of the rf magnetic field: points—experiment, solid line—theory.

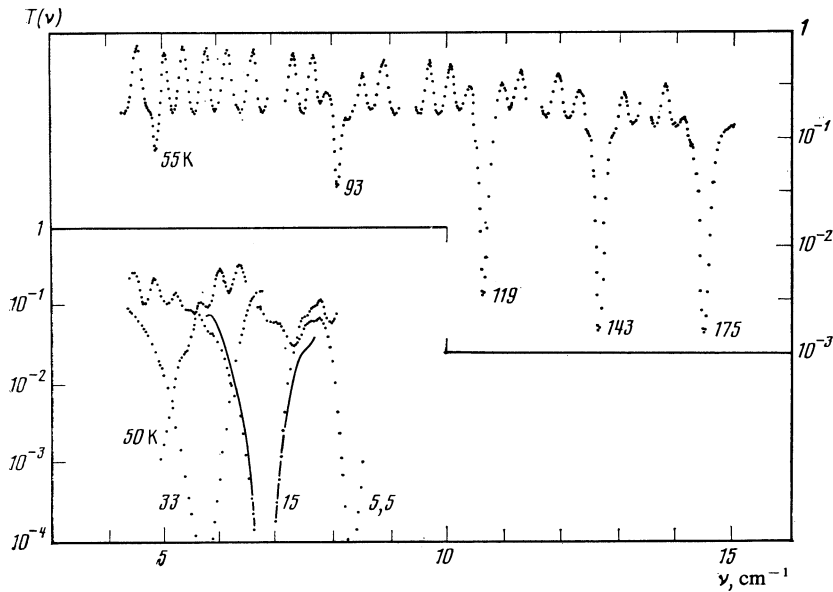


FIG. 2. Transmission spectra of DyFeO₃ for $\mathbf{h}\parallel c$ at various temperatures (in °K).

where $c = 3 \cdot 10^{10}$ cm/s.

The model $T(\nu) = T(\nu, d, \epsilon(\nu), \mu(\nu))$ was fitted to the experimental plots of $T(\nu)$ in two stages. Polynomials for $\epsilon'(\nu)$ and $\epsilon''(\nu)$ were first tried at $\mu = 1$ outside the absorption lines to match the oscillatory experimental $T(\nu)$ curves. These polynomials were next interpolated into the region of the resonances. With ϵ' and ϵ'' so determined in the single-oscillator approximation for $\mu(\nu)$, the absorption lines of the $T(\nu)$ spectrum were next processed and their parameters ν_0 , Γ , and $\Delta\mu_0$ determined. In most cases our measured $T(\nu)$ spectra were described by the theoretical curves to within plotting accuracy (see Fig. 1).

The measurements of the $T(\nu)$ spectra, the succeeding data reduction, and the calculation of the parameters ν_0 , Γ , and $\Delta\mu_0$ for both AFMR modes were carried out in the temperature interval from 4.2 to 600 K. Figure 2 shows typical

experimental $T(\nu)$ curves for $\mathbf{h}\parallel c$ (quasiantiferromagnetic mode) at temperatures above and below the transition point. It can be seen that the line broadens greatly and its intensity increases on going into the antiferromagnetic phase $\Gamma_1(G_y)$.

The temperature dependences obtained from the $T(\nu)$ spectra for the resonance frequencies $\nu_0^{(1,2)}$, for the static contributions $\Delta\mu_0^{(1,2)}$ of the mode to the magnetic permeability, and for the line widths $\Gamma^{(1,2)}$, are shown in Figs. 3–5. It can be seen from Fig. 3 that in DyFeO₃, just as in YFeO₃ (Ref. 8), at high temperature the frequency $\nu_0^{(2)}$ of the quasiantiferromagnetic mode in the $\Gamma_4(G_x F_z)$ phase is higher than the frequency $\nu_0^{(1)}$ of the antiferromagnetic mode. In DyFeO₃ at room temperature $\nu_0^{(1)} = (12.67 \pm 0.04)$ cm⁻¹ and $\nu_0^{(2)} = (17.0 \pm 0.04)$ cm⁻¹.³⁾ With decreasing temperature, however, the frequency $\nu_0^{(2)}$ decreases sharply, crosses $\nu_0^{(1)}$, and reaches a minimum at the phase-transition point $T_M \approx 50$ K.

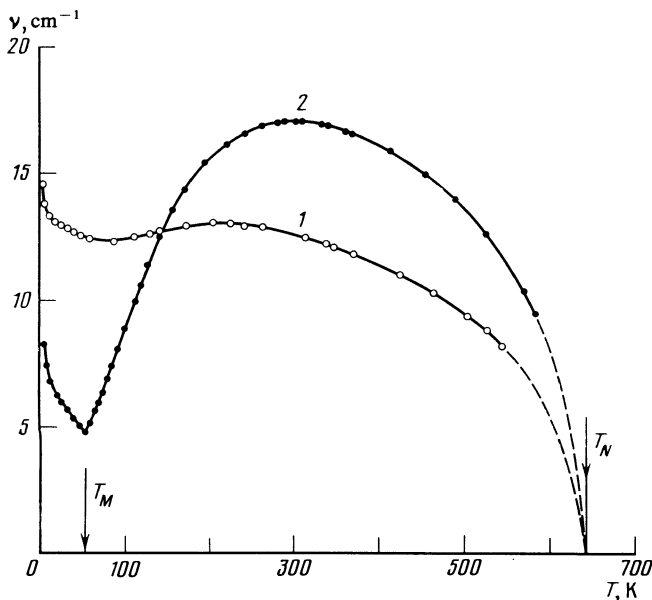


FIG. 3. Temperature dependence of AFMR frequencies in DyFeO₃: 1— $\nu_0^{(1)}$ (quasiferromagnetic mode, $\mathbf{h}\perp c$); 2— $\nu_0^{(2)}$ (quasiantiferromagnetic mode, $\mathbf{h}\parallel c$).

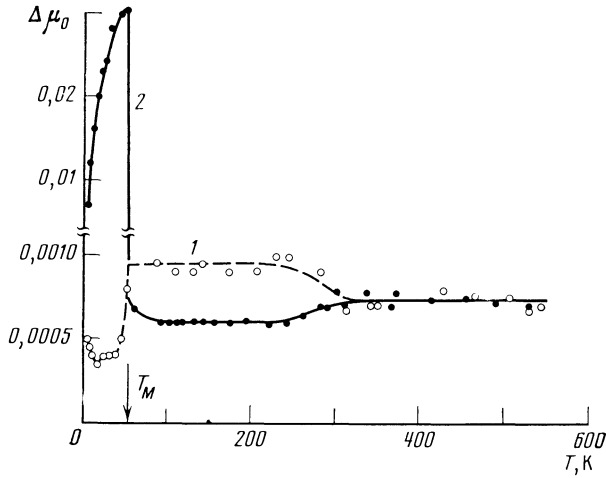


FIG. 4. Temperature dependence of static contribution of two AFMR modes to the magnetic permeability: 1— $\Delta\mu_0^{(1)}$; 2— $\Delta\mu_0^{(2)}$.

This behavior of the frequency $\nu_0^{(2)}$ is evidence of a decrease in the anisotropy energy in the ab plane with decreasing temperature. As for the frequency $\nu_0^{(1)}$ of the quasiferromagnetic mode, it has no noticeable anomaly at the phase-transition point.

The strongest anomalies at orientational PT points occur in the values of $\Delta\mu_0^{(1,2)}(T)$ and $\Gamma^{1,2}(T)$ (Figs. 4 and 5). Their characteristic features are strongly pronounced discontinuities at $T = T_M$, which attest to a change of the system's magnetic configuration. Thus, $\Delta\mu_0^{(2)}$ increases at the point T_M from $7 \cdot 10^{-4}$ to $300 \cdot 10^{-4}$, while the line width $\Gamma^{(2)}$ increases from 0.1 to 0.77 cm^{-1} . Discontinuities are observed also on the temperature dependences of ϵ' and ϵ'' .

The discontinuities of $\Delta\mu_0^{(1,2)}$ and $\Gamma^{(1,2)}$ observed at $T = T_M$ and the fact that the frequency $\nu_0^{(2)}(T)$ of the quasiantiferromagnetic mode is damped at only one temperature indicate that the spins in DyFeO_3 are reoriented via a first-order PT. This agrees with the results of static measurements.¹⁴

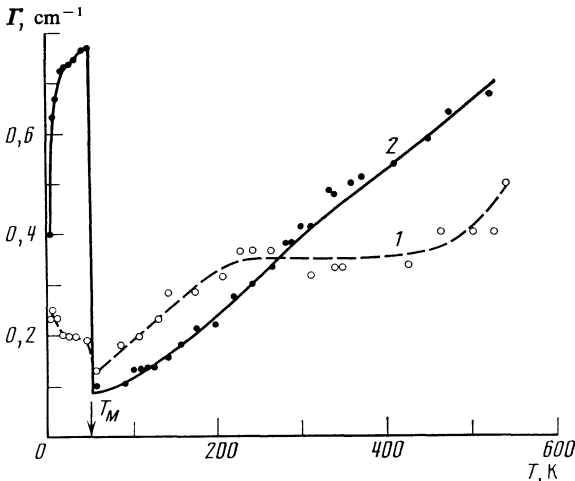


FIG. 5. Temperature dependence of line widths of two AFMR modes: 1— $\Gamma^{(1)}$; 2— $\Gamma^{(2)}$.

3. THEORY AND DISCUSSION OF RESULTS

The main factor that determines qualitatively the magnetic behavior of DyFeO_3 is the exchange interaction of the antiferromagnetically ordered Fe^{3+} ions with the Dy^{3+} ion subsystem. Since the R system is paramagnetic at $T > 3.5 \text{ K}$, its magnetic state is uniquely determined by the effective fields produced by the Fe^{3+} ions. This allows us to eliminate in succession, when describing the static magnetic properties of DyFeO_3 , the variables of the R subsystems from the thermodynamic potential (TP) and express them in terms of the Fe-subsystem basis vectors. The effective (renormalized) TP obtained in this manner, which depends only on the Fe-subsystem variables, is of the form^{1,19}

$$\begin{aligned} \Phi(\mathbf{F}, \mathbf{G}) = & \frac{1}{2} A \mathbf{F}^2 + \frac{1}{2} K_{ac} G_z^2 + \frac{1}{2} K_{ab} G_y^2 + \frac{1}{4} K_2 G_z^4 \\ & + \frac{1}{4} K_2' G_y^4 + \frac{1}{2} K_2'' G_y^2 G_z^2 \\ & - d_1 F_x G_z - d_3 F_z G_x - M_0 \sum_{i=x,y,z} (1 + \eta_i) F_i H_i \\ & - \tau_1 H_x G_x - \tau_3 H_z G_x - \frac{1}{2} \sum_i \chi_R^i H_i^2, \end{aligned} \quad (3)$$

where $\mathbf{F} = (\mathbf{M}_1 + \mathbf{M}_2)/2M_0$ and $\mathbf{G} = (\mathbf{M}_1 - \mathbf{M}_2)/2M_0$ are the dimensionless ferro- and antiferromagnetism vectors, while $\mathbf{M}_{1,2}$ are the magnetic moments of the Fe sublattices and M_0 is the Fe-sublattice saturation magnetic moment ($\sim 5 \mu_B$ per Fe^{3+} ion). The presence of the paramagnetic R subsystem in (3) renormalizes the Fe subsystem's initial TP coefficients, thereby making them strongly temperature-dependent, and gives rise to some new terms. Thus, the coefficients $\tau_{1,3}$ and η_i in (3) are due exclusively to R-Fe interaction. Specific expressions for the TP coefficients for DyFeO_3 are given in Refs. 1 and 19. Minimizing the TP (3) with respect to \mathbf{F} , recognizing that $\mathbf{F} \cdot \mathbf{G} = 0$ and $\mathbf{G}^2 = 1 - \mathbf{F}^2 \approx 1$, we eliminate \mathbf{F} from the TP and represent it in the form⁴⁾

$$\begin{aligned} \Phi(\mathbf{G}) = & \frac{1}{2} K_{ac}^{\text{eff}} G_z^2 + \frac{1}{2} K_{ab}^{\text{eff}} G_y^2 + \frac{1}{4} K_{2 \text{ eff}} G_z^4 + \frac{1}{4} K_{2 \text{ eff}} G_y^4 \\ & + \frac{1}{2} K_{2 \text{ eff}}'' G_y^2 G_z^2 - m_x H_x G_z - m_z H_z G_x - G_x G_z \sum_i m_i' H_i G_i \\ & - \frac{1}{2} \sum_i \chi_{\perp}^i H_i H_k (\delta_{ik} - G_i G_k) - \frac{1}{2} \sum_i \chi_R^i H_i^2, \end{aligned} \quad (4)$$

where

$$K_{ac}^{\text{eff}} = K_{ac} + 2d_3 d_+ / A, \quad K_{ab}^{\text{eff}} = K_{ab} + d_3^2 / A, \quad (5)$$

$$K_{2 \text{ eff}} = K_2 - 2d_+^2 / A, \quad K_{2 \text{ eff}}' = K_2', \quad K_{2 \text{ eff}}'' = K_2'' - d_+^2 / A$$

are effective second- and fourth-order anisotropy constants in which $d_+ = d_1 + d_3$;

$$m_x = \tau_1 + M_0(1 + \eta_x) d_1 / A, \quad m_z = \tau_3 + M_0(1 + \eta_z) d_3 / A \quad (6)$$

are quantities that determine the weakly ferromagnetic moment of the crystal at $\mathbf{H} = 0$ in the phases $\Gamma_2(G_z F_z)$ and $\Gamma_4(G_x F_z)$, respectively

$$\begin{aligned} m_i' = & -M_0(1 + \eta_i) d_+ / A, \quad \chi_{\perp}^{ik} = \chi_{\perp}^0 (1 + \eta_i) (1 + \eta_k), \\ & \chi_{\perp}^0 = M_0^2 / A = M_0 / 2H_E, \\ & \delta_{ik} = 0 \quad \text{at } i \neq k \text{ and } 1 \quad \text{at } i = k. \end{aligned} \quad (7)$$

At $\mathbf{H} = 0$ the equilibrium states of the system are determined by the relations between the effective anisotropy con-

stants. Thus the stability (lability) region of the weakly ferromagnetic phase $\Gamma_4(G_x F_z)$ is determined by the conditions

$$\Phi_{\theta\theta^0} = K_{ac}^{\text{eff}} > 0, \quad \Phi_{\varphi\varphi^0} = K_{ab}^{\text{eff}} > 0,$$

and that of the antiferromagnetic phase $\Gamma_1(G_y)$ by the condition

$$\Phi_{\theta\theta^0} = K_{ac}^{\text{eff}} + K_{2\text{eff}}'' - K_{ab}^{\text{eff}} - K_{2\text{eff}}' > 0, \quad \Phi_{\varphi\varphi^0} = -K_{ab}^{\text{eff}} - K_{2\text{eff}}' > 0.$$

Thus, when the sign of K_{ab}^{eff} is reversed the phase Γ_4 becomes unstable and an orientational transition $\Gamma_4(G_x F_z) \rightarrow \Gamma_1(G_y)$ takes place. In DyFeO₃, according to experiment, this transition is of first order, i.e. $K_{2\text{eff}}' < 0$. The temperature of this transition is determined from the condition that the TP of the phases Γ_4 and Γ_1 be equal: $K_{ab}^{\text{eff}}(T_M) + \frac{1}{2}K_{2\text{eff}}' = 0$.

We consider now the dynamic properties of DyFeO₃. To describe the main observable singularities of the behavior of the resonance frequencies and of the components of the high-frequency magnetic-susceptibility tensor, we use a simplified model based on analysis of the dynamics of the magnetic moments of the Fe subsystem with the aid of the Landau-Lifshitz equations:

$$\frac{1}{\gamma} \dot{\mathbf{F}} = -[\mathbf{F} \times \mathbf{H}_F] - [\mathbf{G} \times \mathbf{H}_G], \quad \frac{1}{\gamma} \dot{\mathbf{G}} = -[\mathbf{G} \times \mathbf{H}_F] - [\mathbf{F} \times \mathbf{H}_G], \quad (8)$$

where γ is the gyromagnetic ratio, and $\mathbf{H}_F = -M_0^{-1} \partial \Phi / \partial \mathbf{F}$ and $\mathbf{H}_G = -M_0^{-1} \partial \Phi / \partial \mathbf{G}$ are the effective fields calculated on the basis of the TP (3). The influence of the rare-earth ions on the dynamics of the Fe subsystem is taken into account here only via the TP (3) which is renormalized by the R-Fe interaction. This approach yields a direct connection between the principal dynamic properties of the system with the static ones determined by the TP (3) and (4). The range of validity of this approximation and some additional dynamic effects connected with the R subsystem will be discussed below.

Linearizing and solving Eqs. (8), we obtain the following expressions for the resonant frequencies $\nu_0^{(1,2)}$ and the components $\chi_{ik}^{(v)}$ of the high-frequency magnetic-susceptibility tensor (at $\mathbf{H} = 0$):

a) the phase $\Gamma_4(G_x F_z)$ ($T > T_M$):

$$\nu_0^{(1)} = (\gamma/2\pi) [2H_E(K_{ac}^{\text{eff}}/M_0)]^{1/2}, \quad (9)$$

$$\nu_0^{(2)} = (\gamma/2\pi) [2H_E(K_{ab}^{\text{eff}}/M_0)]^{1/2},$$

$$\hat{\chi}(\nu) = \begin{pmatrix} \chi_{xx} & \chi_{xy} & 0 \\ \chi_{yx} & \chi_{yy} & 0 \\ 0 & 0 & \chi_{zz} \end{pmatrix} \quad (10)$$

where

$$\begin{aligned} \chi_{xx} &= \chi_{xx}^0 N^{(1)}(\nu), \quad \chi_{yy} = \chi_{\perp}^{yy} N^{(1)}(\nu), \\ \chi_{xy} &= -\chi_{yx} = -i(\nu/\nu_0^{(1)}) (\chi_{xx} \chi_{yy})^{1/2} \\ \chi_{zz} &= \chi_{\perp}^{zz} N^{(2)}(\nu), \quad \chi_{xx}^0 = (m_x + m_x')^2 / K_{ac}^{\text{eff}}, \\ N^{(r)}(\nu) &= (\nu_0^{(r)})^2 / [(\nu_0^{(r)})^2 - \nu^2 + i\nu\Gamma^{(r)}], \quad r=1, 2; \end{aligned} \quad (11)$$

b) the phase $\Gamma_1(G_y)$ ($T < T_M$)

$$\nu_0^{(1)} = (\gamma/2\pi) [2H_E(K_{ac}^{\text{eff}} + K_{2\text{eff}}'' - K_{ab}^{\text{eff}} - K_{2\text{eff}}')/M_0]^{1/2}, \quad (12)$$

$$\nu_0^{(2)} = (\gamma/2\pi) [2H_E(-K_{ab}^{\text{eff}} - K_{2\text{eff}}')/M_0]^{1/2},$$

$$\hat{\chi}(\nu) = \begin{pmatrix} \chi_{xx} & 0 & 0 \\ 0 & \chi_{yy} & 0 \\ 0 & 0 & \chi_{zz} \end{pmatrix}, \quad (13)$$

where

$$\begin{aligned} \chi_{xx} &= (\chi_{xx}^{0'} + \chi_{\perp}^{xx}) N^{(1)}(\nu), \\ \chi_{yy} &= 0, \quad \chi_{zz} = (\chi_{zz}^{0'} + \chi_{\perp}^{zz}) N^{(2)}(\nu), \\ \chi_{xx}^{0'} &= m_x^2 / (K_{ac}^{\text{eff}} + K_{2\text{eff}}'' - K_{ab}^{\text{eff}} - K_{2\text{eff}}'), \\ \chi_{zz}^{0'} &= m_z^2 / |K_{ab}^{\text{eff}} + K_{2\text{eff}}'|. \end{aligned} \quad (14)$$

The quantities $\chi_1^{xx}, \chi_1^{yy}, \chi_1^{zz}$ are defined in Eq. (7). Damping is taken into account in the high-frequency magnetic susceptibility by introducing additional phenomenological coefficients $\Gamma^{(1,2)}$ that determine the width of the corresponding AFMR line.

Let us analyze the experimental results on the basis of the equations given for $\nu_0^{(1,2)}$ and $\hat{\chi}(\nu)$. We note first that the observed damping of the frequency $\nu_0^{(2)}(T)$ as the phase-transition point is approached reflects, according to (9) and (12), the temperature dependence of the anisotropy constant $K_{ab}^{\text{eff}}(T)$ which reverses sign near TM. At the transition point ($K_{ab}^{\text{eff}}(T_M) = -K_{2\text{eff}}'/2$) the frequency of the soft mode is finite and continuous, but its slope $d\nu_0^{(2)}/dT$ reverses sign. The frequency at the transition point

$$\nu_0^{(2)}(T_M) = (\gamma/2\pi) [2H_E(-K_{2\text{eff}}'/2M_0)]^{1/2} \quad (15)$$

is determined by a fourth-order effective anisotropy constant, so that $K_{2\text{eff}}'$ can be directly estimated if $\chi_1^0 = M_0/2H_E$ is known. The latter can be easily estimated from the values of $\Delta\mu_0^{(2)}$ measured for the antiferromagnetic mode at $T \sim 300$ K, when $\eta_{zz} \gg 1$ and $\chi_1^{zz} \approx \chi_1^0$. As a result, putting $\Delta\mu_0^{(2)} = 7 \cdot 10^{-4}$ (see Fig. 4), $\chi_1^0 = \Delta\mu_0^{(2)}/4\pi\rho = 0.7 \cdot 10^{-5}$ cm³/g ($\rho \approx 8.0$ g/cm³ is the density of DyFeO₃), and $\gamma = 1.76 \cdot 10^7$ Hz/Oe we get $K_{2\text{eff}}' = 3.5 \cdot 10^4$ erg/g, which agrees with the data of Ref. 1 ($K_{2\text{eff}}' = 2 \cdot 10^4$ erg/g).

The frequency $\nu_0^{(1)}$ of the other mode has at the transition point, according to (9) and (12), a discontinuity equal to

$$\begin{aligned} \nu_0^{(1)}(T_M^-) - \nu_0^{(1)}(T_M^+) &= (\gamma/2\pi) (2H_E/M_0)^{1/2} \\ &\times [(K_{ac}^{\text{eff}} + K_{2\text{eff}}'' - K_{2\text{eff}}'/2)^{1/2} - (K_{ac}^{\text{eff}})^{1/2}] \end{aligned} \quad (16)$$

Failure to observe this discontinuity in experiment (see Fig. 3) indicates that $|K_{2\text{eff}}''| \sim |K_{2\text{eff}}'| \ll K_{ac}^{\text{eff}}$. This is indeed the case for DyFeO₃ at $T \sim \text{TM}$.

We consider now the behavior of the magnetic permeability tensor in a Morin-type phase transition. The largest discontinuity is observed here in the component $\Delta\mu_{zz}^0 \equiv \Delta\mu_0^{(2)}$ of the static contribution to the magnetic permeability. According to (10), (11), (13), and (14) we get

$$\frac{1}{4\pi\rho} [\Delta\mu_0^{(2)}(T_M^-) - \Delta\mu_0^{(2)}(T_M^+)] = \chi_{zz}^{0'}(T_M). \quad (17)$$

The quantity $\chi_{zz}^{0'}$ is the static differential susceptibility in the

antiferromagnetic phase $\Gamma_1(G_y)$ relative to spin rotation in the ab plane, and is inversely proportional to the anisotropy constant in this plane. Since the anisotropy constant decreases at the PT point, this causes a large jump of the susceptibility on going over to the Γ_1 phase. In contrast to the antiferromagnetic phase Γ_1 , the susceptibility along the z axis above the PT point, i.e., in the Γ_4 phase, is independent of K and is determined only by the value of χ_T^{zz} [see Eq. (11)], and it is this which makes it small. Knowing the susceptibility jump at the PT point ($\chi_{zz}^{0'}(T_M) = 3.1 \cdot 10^{-4}$ cm³/g) and the value of $K'_{2\text{eff}}$ we can estimate the weakly ferromagnetic moment along the c axis, viz., $m_z = 2.3$ G cm³/g = $0.11 \mu_B$ /ion; this agrees with the data of Refs. 13 and 14.

The antiferromagnetic-mode jump $\Delta\mu_0^{(1)}$ observed at the PT point likewise agrees qualitatively with the model considered. The fact that in the antiferromagnetic phase Γ_1 the observed value of $\Delta\mu_0^{(1)}$ does not vanish, as it should according to (13) and (14) at $\mathbf{h} \parallel \mathbf{b}$, can be due to an inaccurate orientation of the sample or to a contribution of the parallel susceptibility (χ_{\parallel}^{pp}) of the Fe subsystem to $\Delta\mu_0^{(1)}$.

Besides the Morin PT temperature, DyFeO₃ has one more singular point, $T_0 \approx 150$ K, at which the frequencies of the quasiferromagnetic and quasiferromagnetic modes cross (see Fig. 3). According to (9), the effective anisotropy constants in the ac and ab planes become equalized at this temperature. This manifests itself in the static magnetic properties as a restructuring of the domain walls, viz., at $T > T_0$ ($K_{ab}^{\text{eff}} > K_{ac}^{\text{eff}}$) the stable domain wall is the one with rotation of the ac -plane spins (its energy is $\sigma_{ac} \sim (K_{ac}^{\text{eff}})^{1/2}$), and at $T < T_0$ ($K_{ab}^{\text{eff}} < K_{ac}^{\text{eff}}$) the stable wall is the one with spin rotation in the ab plane ($\sigma_{ab} \sim (K_{ab}^{\text{eff}})^{1/1}$). Restructuring of the domain walls in DyFeO₃ was observed by the NMR method in Ref. 20 at $T \sim 150$ K.

We discuss now in greater detail the role of the dynamics of the Dy³⁺ subsystem in the DyFeO₃ properties observed by us. We have already noted that the oscillations of the Fe and R subsystems are coupled by virtue of the R–Fe interaction. The model used above is in fact the quasistatic limiting case of allowance for this coupling, wherein the magnetic moments of the R subsystem follow “instantaneously” the magnetic moments of the Fe³⁺ ions. The renormalized TP (3) can be used in this case to describe the dynamics of the variables F and G . Obviously, the condition for the validity of this approximation is $\nu_R^{(i)} \gg \nu_0^{(1,2)}$, where $\nu_R^{(i)}$ are the R-subsystem resonant frequencies corresponding to various transitions between the energy levels of the ground multiplet R^{3+} split by the crystal and exchange fields.⁵⁾ The dynamic susceptibility of the rare-earth ion differs little then from its static susceptibility.

The Dy³⁺-ion spectrum in the crystal field consists of doublets with energies $E_1 = 0$, $E_2 = 52$ cm⁻¹, $E_3 = 147$ cm⁻¹, etc. (Ref. 21). The exchange and dipole R–Fe interactions give rise to a doublet splitting, but a small one (~ 1 cm⁻¹) and even zero for the lower Dy³⁺ doublet in phases Γ_4 and Γ_1 . Thus, the resonant frequencies $\nu_R^{(i)}$ connected with the doublet splitting are small compared with $\nu_0^{(1,2)}$, but the frequencies due to transitions between different doublets, on the contrary, substantially exceed $\nu_0^{(1,2)}$.

A characteristic feature of DyFeO₃ is that the principal

role in the formation of its static magnetic properties is played by the shift of the “centroids” of the Dy³⁺-ion doublets by the R–Fe interaction (\mathcal{H}_{R-Fe}). This shift is determined by the matrix elements of the operator \mathcal{H}_{R-Fe} between the wave functions of the different doublets and by the distances between them.^{1,19} It reverses, in particular, the sign of the anisotropy constant K_{ab}^{eff} and determines the appreciable contribution of the Dy³⁺ subsystem to the magnetization m_z and to the susceptibility χ_R^{zz} . This means that an equally important role will be played by transitions between different Dy³⁺ doublets having frequencies $\nu_R^{(i)} \gg \nu_0^{(1,2)}$. This justifies the use of the model above. We note, however, that this applies to a greater degree to the quasiantiferromagnetic mode, whose parameters (τ_3 , η_{zz} etc.) receive rare-earth contributions determined by the matrix elements of the operator \mathcal{H}_{R-Fe} between the ground and excited doublets.^{1,19} The foregoing estimates and a comparison with the static magnetic characteristics confirm this conclusion.

As for the quasiferromagnetic mode, the model is apparently only partially applicable (at high temperatures). The point is that the quasiferromagnetic-mode parameters contribute to transitions between two states of the lower doublet (or of other doublets) of the Dy³⁺ ion. Since their frequencies $\nu_R^{(i)}$ are low, their contribution to the dynamic susceptibility at $\nu \gg \nu_R^{(i)}$ is negligibly small compared with its static value. This should lead at low temperatures to some deviation of the quasiferromagnetic-mode parameters from their values (12)–(14) calculated within the framework of the approximation used above and based on the TP (3), (4). This deviation is negligible at high temperatures ($T \gtrsim 50$ K), as attested by the fact that the crossing of the frequencies $\nu_0^{(1)}$ and $\nu_0^{(2)}$, which we observed, occurs at the same temperature at which the restructuring of the domain walls is observed.²⁰ In view of this, we can use in the calculations of the DyFeO₃ anisotropy constants the resulting temperature dependences of the frequencies $\nu_0^{(1)}$ and $\nu_0^{(2)}$, as well as the value of χ_1^0 . Their temperature dependences are shown in Fig. 6.

We call attention to the appreciable growth of the anisotropy constants (and of the corresponding resonant frequencies in Fig. 4) at helium temperatures. The temperature dependence of the threshold field $H_{\text{thr}}^c(T)$ that induces the $\Gamma_1 \rightarrow \Gamma_4$ transition^{1,14} and is proportional to K_{ab}^{eff} is similar. These data do not fit the DyFeO₃ model used in Refs. 1 and 19, according to which K_{ac}^{eff} should decrease at low temperatures and K_{ab}^{eff} is independent of temperature. A possible cause of the observed behavior of the anisotropy constants is the additional contribution made by impurity ions (such as Al³⁺) or defects, to which DyFeO₃, as shown in Ref. 22, is very sensitive.

With regard to the peculiarities of the behavior of the AFMR line widths (see Fig. 5), it should be noted that here, just as in the static properties of DyFeO₃, an important role is played by the rare-earth subsystem, which is apparently one of the main relaxation channels of the Fe-subsystem spin excitations. Thus, the discontinuities of $\Gamma^{(1,2)}$ at the Morin point can be due to a change in the rate of this relaxation as a result of the change of the magnitude (amplitude) of the interaction between the Fe³⁺ and Dy³⁺ ions in the course of reorientation. Another peculiarity of $\Gamma^{(1,2)}(T)$ appears at he-

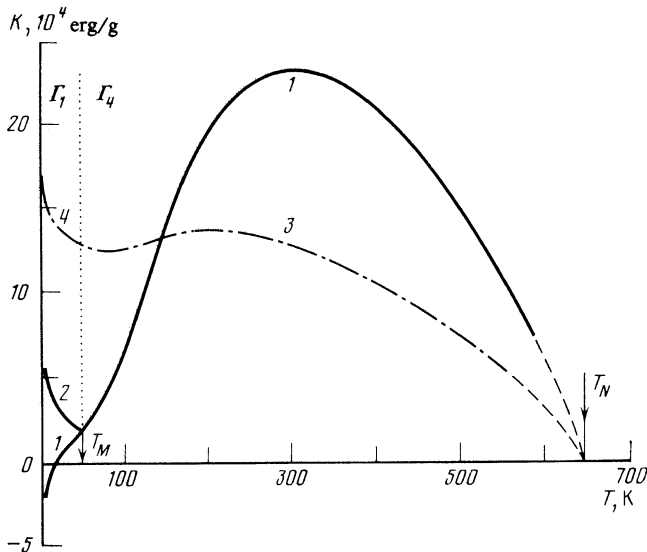


Fig. 6. Temperature dependence of DyFeO₃ anisotropy constants: 1— K_{ab}^{eff} ; 2— $|K_{ab}^{\text{eff}} + K_{2\text{eff}}^{\text{eff}}|$; 3— K_{ac}^{eff} ; 4— $K_{ac}^{\text{eff}} + K_{2\text{eff}}^{\text{eff}} - K_{ab}^{\text{eff}} - K_{2\text{eff}}^{\text{eff}}$.

lium temperatures. The reason is the difference in the character of this dependence with decreasing temperature ($\Gamma^{(1)}$ increases and $\Gamma^{(2)}$ decreases). A possible cause of this behavior of $\Gamma^{(1,2)}$ is the approach to the point of antiferromagnetic ordering of the Dy subsystem ($T_{N2} = 3.5$ K), in conjunction with the strongly anisotropic (Ising) properties of the Dy³⁺ ions at low temperatures.

4. CONCLUSION

We summarize our results.

Two AFMR modes were observed in the submillimeter-transmission spectra of DyFeO₃, quasiferromagnetic and quasiantiferromagnetic. Measurements of the DyFeO₃ transmission spectra in a wide range of frequencies ($\nu = 5\text{--}33$ cm⁻¹) and temperatures ($T = 4.2\text{--}600$ K) yielded the temperature dependences of the AFMR frequencies, of the linewidths, and of the contributions of the corresponding modes to the static magnetic permeability. Anomalous behavior of the parameters of both modes was observed at the points of orientational Morin-type phase transitions. The character of these anomalies indicates that the $\Gamma_4 \rightarrow \Gamma_1$ reorientation proceeds via a first-order PT, thus confirming the results of investigations of the static magnetic properties of DyFeO₃. Crossing of two AFMR modes was observed at $T \sim 150$ K. This is the same temperature at which restructuring of the domain walls was detected by a NMR method.²⁰ The AFMR frequencies $\nu_0^{(1,2)}(T)$ were observed to increase noticeably at liquid-helium temperature.

The static and dynamic magnetic properties of DyFeO₃ were self-consistently described using a TP with parameters renormalized by the R-Fe interaction and using the Landau-Lifshitz equations for a two-sublattice antiferromagnet. It is shown that most observed dynamic properties of DyFeO₃, particularly the behavior of $\nu_0^{(2)}(T)$ and $\Delta\mu_0^{(2)}(T)$, agree well with the model employed and with the static magnetic properties of the system. The values obtained for $\nu_0^{(1,2)}(T)$ and $\Delta\mu_0^{(1,2)}(T)$ can be used to extract additional information on the parameters of the magnetic interactions in the system. In

particular, they permit direct determination of the anisotropy constants and identify the contribution to them from the rare-earth system. The values of $\Delta\mu_0^{(1,2)}$ can yield such characteristics as the transverse susceptibility and the Fe-subsystem spin-rotation susceptibility, which are difficult to determine from purely static magnetic measurement because of the large contribution of the rare-earth ions to the susceptibility of the system.

We are grateful to G. V. Kozlov and A. K. Zvezdin for a discussion of the work and for a number of valuable remarks.

¹For example, in the $\Gamma_4(G_x F_z)$ phase, in which the antiferromagnetism vector \mathbf{G} is directed along the a axis and the weak-ferromagnetism vector \mathbf{F} along the c axis, the oscillating quantities are F_x , F_y , and G_z in the quasiferromagnetic mode and F_z , G_x , and G_y in the quasiantiferromagnetic mode (two-sublattice approximation).

²BWO—backward-wave oscillator.

³The AFMR frequencies in DyFeO₃ measured in Ref. 4 at room temperature by a Raman-scattering method were $\nu_0^{(1)} = 9.1$ cm⁻¹ and $\nu_0^{(2)} = 16.5$ cm⁻¹. Their values, however, differ somewhat from ours by amounts exceeding our experimental error.

⁴Since we are considering the behavior of the system at relatively low temperatures ($T \lesssim T_N/2$), the Fe-sublattice magnetic moments can be regarded as saturated, i.e., $|\mathbf{M}_1| = |\mathbf{M}_2| = M_0$ or $\mathbf{F}^2 + \mathbf{G}^2 = 1$, $\mathbf{F} \cdot \mathbf{G} = 0$.

⁵We note that rare-earth modes can also be relaxational. In this case the AFMR frequencies $\nu_0^{(1,2)}$ must be compared with the characteristics of the relaxational frequencies of the rare-earth subsystem.

¹K. P. Belov, A. K. Zvezdin, A. M. Kadomtseva, and R. Z. Levitin, *Orientatsionnye perekhody v redkozemel'nykh magnetikakh* (Orientational Transitions in Rare-Earth Magnets), Nauka, 1979.

²R. C. LeCraw, R. Wolf, E. M. Georgy, F. B. Hagedorn, J. C. Hensel, and J. P. Remeika, *J. Appl. Phys.* **39**, 1019 (1968).

³S. M. Shapiro, J. D. Axe, and J. P. Remeika, *J. Phys.* **B10**, 2014 (1974).

⁴R. M. White, R. J. Nemanich, and C. Herring, *Phys. Rev. B* **25**, 2014 (1982).

⁵K. B. Aring and A. J. Sievers, *J. Appl. Phys.* **41**, 1197 (1970).

⁶V. I. Ozhogin, V. G. Shapiro, K. G. Gurtovoi, E. A. Galst'yan, and A. Ya. Chervonenkis, *Zh. Eksp. Teor. Fiz.* **62**, 2221 (1972) [*Sov. Phys. JETP* **35**, 1162 (1972)].

⁷L. V. Velikov, E. A. Vitvinin, G. E. Ivannikova, F. F. Igoshin, A. P. Kur'yanov, and S. S. Markianov, *Fiz. Tverd. Tela* (Leningrad) **22**, 3612 (1980) [*Sov. Phys. Solid State* **22**, 2115 (1980)].

⁸A. A. Volkov, Yu. G. Goncharov, G. V. Kozlov, K. N. Kocharyan, S. P. Lebedev, A. S. Prokhorov, and A. M. Prokhorov, *Pis'ma Zh. Eksp. Teor. Fiz.* **39**, 140 (1984) [*JETP Lett.* **39**, 166 (1984)].

⁹A. M. Balbashov, G. V. Kozlov, S. P. Lebedev, A. M. Prokhorov, and A. S. Prokhorov, *ibid.* **39**, 461 (1984) [**39**, 560 (1984)].

¹⁰G. F. Hermann, *J. Phys. Chem. Solids* **24**, 597 (1963).

¹¹C. H. Tsang, R. L. White, and R. M. White, *J. Appl. Phys.* **49**, 6063 (1978).

¹²V. G. Bar'yakhtar, I. M. Vitebskiĭ, and D. A. Yablonskiĭ, *Zh. Eksp. Teor. Fiz.* **76**, 1381 (1979) [*Sov. Phys. JETP* **49**, 703 (1979)].

¹³G. Gorodetsky, B. Sharon, and S. Shtrikman, *J. Appl. Phys.* **39**, 1371 (1968).

¹⁴K. P. Belov, A. K. Zvezdin, A. M. Kadomtseva, and I. B. Krynetskiĭ, *Zh. Eksp. Teor. Fiz.* **67**, 1974 (1974) [*Sov. Phys. JETP* **40**, 980 (1975)].

¹⁵A. M. Balbashov, A. Ya. Chervonenkis, A. V. Antonov, and V. E. Bakhtluzov, *Izv. AN SSSR, ser. fiz.* **35**, 1243 (1971).

¹⁶A. A. Volkov, Yu. G. Goncharov, G. V. Kozlov, S. P. Lebedev, and V. I. Mal'tsev, *Prib. Tekh. Eksp. No. 2*, 236 (1984).

¹⁷G. V. Kozlov, A. A. Volkov, and S. P. Lebedev, *Usp. Fiz. Nauk* **133** (1981) [*Sov. Phys. Usp.* **24**, 916 (1981)].

¹⁸L. M. Brekhovskikh, *Waves in Layered Media*, Academic, 1960.

¹⁹A. K. Zvezdin and V. M. Matveev, *Zh. Eksp. Teor. Fiz.* **77**, 1076 (1979) [*Sov. Phys. JETP* **50**, 543 (1979)].

²⁰A. V. Zaleskiĭ, A. M. Savvinov, I. S. Zheludev, and A. N. Ivashchenko, *ibid.* **68**, 1449 (1975) [**41**, 723 (1975)].

²¹H. Schuchert, S. Hufner, and R. Faulhaber, *Z. Phys.* **220**, 273 (1969).

²²A. M. Kadomtseva, A. K. Zvezdin, M. M. Lukina, V. N. Milov, A. A. Mukhin, and T. L. Ovchinnikova, *Zh. Eksp. Teor. Fiz.* **73**, 2324 (1977) [*Sov. Phys. JETP* **46**, 1216 (1977)].

Translated by J. G. Adashko